

Experimental study of wall boundary conditions for Large Eddy Simulation

G. J. Kunkel¹, I. Marusic¹ and F. Porté-Agel²

¹Department of Aerospace Engineering and Mechanics
 University of Minnesota, Minneapolis, MN 55455, USA

²St. Anthony Falls Laboratory
 University of Minnesota, Minneapolis, MN 55414, USA

Abstract

Three conventional Large Eddy Simulation (LES) boundary conditions, based on the instantaneous filtered velocity, are tested using simultaneously measured values of filtered wall shear stress and filtered velocities, at locations nominally within the log region of a turbulent boundary layer at $Re_\theta = 3500$. The data was collected using arrays of hot-film wall shear stress sensors and \times -wire velocity probes. The models based on the streamwise component velocity perform better than those which use the wall-normal component. A new model, also based on the streamwise component of velocity, is proposed which more accurately describes the shear stress measured at the wall. The new model is expected to be more applicable over a larger range of Reynolds number and wall normal positions within the logarithmic region because of its agreement with the ‘outer-flow’ scaling similarity of the streamwise component of velocity spectra.

Introduction

Recently a workshop [1] was conducted to discuss some of the difficulties facing LES and the role of experimentation in overcoming them. One of these difficulties is the modelling of the wall boundary condition. In an LES of a high Reynolds number boundary layer the grid size is large compared to the smallest scales of the flow and thus the first grid point in the simulation is usually in the logarithmic region. Therefore, the sublayer is not resolved and the boundary condition must account for effects of this poor resolution. To account for this, the no slip boundary condition is often replaced with a condition on the wall shear stress based on the correlation of the fluctuations of wall shear stress and velocity at the first grid point above the wall.

This study considers the (1,3) component of three wall shear stress models currently used in LES, where 1,2,3 represent the streamwise (x), spanwise (y), and wall-normal (z) directions respectively. The three models analyzed were developed by Schumann [10], Grötzbach [2] and Piomelli, Ferziger & Moin [7] and following the convention of [7] will be referred to as the ‘SG’, ‘shifted SG’, and ‘ejection’ models. These models were analyzed in [7] where the shifted SG and ejection models were found to perform best based on results from a DNS of a turbulent channel flow at $Re_\tau = U_\tau \delta / \nu = 640$, where δ is channel half-width, U_τ is wall shear velocity and ν is kinematic viscosity. Note that these three models assume that a standard logarithmic law exists and have been used extensively in attached boundary layer calculations.

For this experimental study, an attached, nominally zero pressure gradient, turbulent boundary layer at $Re_\tau = 1350$ is considered. The modelled wall shear stress, obtained from the filtered velocity components from three

\times -wires, is compared to the filtered wall shear stress obtained from nine wall shear stress hot-film sensors. The models are compared based on qualitative observations of the shear stress signatures along with quantitative statistical analyses of correlation coefficients and wall shear stress energy spectra. Based on the results from these comparisons a new model is proposed.

Existing wall shear stress models

A basic wall shear stress model used in LES is the Schumann - Grötzbach (SG) model,

$$\tau_m(x, y, z, t) = \left[\frac{\langle \tau_w \rangle}{\langle \bar{u}(x, y, z, t) \rangle} \right] \bar{u}(x, y, z, t), \quad (1)$$

where $\langle \rangle$ denotes a long time average, $(-)$ signifies the spatial filtering operation, $\langle \tau_w \rangle$ represents the mean wall shear stress and τ_m represents the instantaneous modelled wall shear stress. All wall shear stresses are kinematic stresses and the sign convention is the same as that used in LES (the mean wall shear stress, $-\langle \tau_w \rangle$, has a positive value). Schumann [10] used this condition in a DNS of a turbulent channel flow where $\langle \bar{u}(x, y, z) \rangle$ was determined using the logarithmic law of the wall while $\langle \tau_w \rangle$ was obtained from the driving pressure gradient of the channel. Grötzbach [2] used the same model except for $\langle \bar{u}(x, y, z) \rangle$ the average velocity over a plane at position z parallel to the wall was used while the log. law was used to determine $\langle \tau_w \rangle$.

To better correlate the instantaneous fluctuations in the wall shear stress with the instantaneous fluctuations in the velocity at the first grid point above the wall the shifted SG model incorporates a shift in the filtered velocity signature,

$$\tau_m(x, y, z, t) = \left[\frac{\langle \tau_w \rangle}{\langle \bar{u}(x, y, z, t) \rangle} \right] \bar{u}(x + \Delta_s, y, z, t), \quad (2)$$

where Δ_s is the streamwise displacement. This modification agrees well with the theory of inclined coherent structures along the wall in the turbulent boundary layer. The displacement can be found from experiments or DNS and [7] suggest using $\Delta_s = (1 - |z|) \cot(8^\circ)$ for $30 < z^+ < 50-60$, and that at larger distances from the wall 13° should be used.

In an attempt to better describe the sweeping and ejection events of vortex structures along the wall in a turbulent boundary layer the ejection model uses the wall-normal component of the fluctuating velocity such that

$$\tau_m(x, y, z, t) = \langle \tau_w \rangle + CU_\tau \bar{w}(x + \Delta_s, y, z, t), \quad (3)$$

where U_τ , the wall shear velocity, is equal to $(-\langle \tau_w \rangle / \rho)^{\frac{1}{2}}$ (ρ is the density of the fluid). \bar{w} represents the filtered



Figure 1: View of experimental setup. (Flow is from left to right)

wall-normal velocity component, and C is a dimensionless constant of order 1. It was suggested that the wall-normal velocity would better describe the fluctuating shear stress at the wall.

Experimental method

Data was obtained in a boundary layer wind tunnel with nominally zero streamwise pressure gradient where the working section was 1.2 m wide, 4.7 m long, and nominally 0.3 m high. Measurements were made 3.2 m downstream of a trip-wire where the boundary layer thickness $\delta = 64$ mm. The Reynolds number based on momentum thickness $R_\theta = U_1\theta/\nu = 3500$ where θ is momentum thickness and $U_1 = 8.9$ m/s is the free stream velocity. The Karman number $Re_\tau = U_\tau\delta/\nu = 1350$.

Instantaneous streamwise wall shear stress components were obtained with nine TSI flush mount hot-film sensors. Figure 1 shows a view of the experimental setup. The sensing films on all the probes were 0.15×1.5 mm (approximately 3×30 viscous wall units). The nine shear sensors were mounted flush with the top of a 76 mm diameter Delrin plug in a 3×3 array with a distance of 6.02 mm between adjacent sensor centres which was then mounted flush to the top of the wind tunnel floor.

Instantaneous streamwise and wall normal velocity components were obtained using three \times -wire velocity probes. The wires were constructed in the laboratory and were $5\mu\text{m}$ copper coated tungsten wires with a 1 mm sensing length. As seen in figure 1 the wires were mounted in an array in the spanwise direction above the most downstream set of hot-film shear sensors. The wall normal wire positions were $z^+ = zU_\tau/\nu = 98, 123, 155, 196, 247, \text{ and } 311$.

The experimental set up is designed to replicate a computational cell immediately above the wall in an actual LES. Following [8] a two-dimensional filter is used to approximate the three-dimensional filter used in an actual LES. Taylor's hypothesis was used with a convection speed of $U_c = 0.82U_1$ at all wall normal positions. A box filter of length $\Delta_F = 18$ mm (approximately 400 wall units) was then applied in the streamwise and spanwise directions to obtain the filtered velocity. In agreement with high Reynolds number simulations, the filtered velocities are calculated at heights where the logarithmic law of the wall holds and the filter size is made larger than the vertical grid spacing. Box, Gaussian, and sharp spectral filters, were all compared in the streamwise direction

but yielded negligible differences in the results. A two-dimensional filter of the same size is applied to the wall shear stress measurements. It is important to note that a two-dimensional distribution of wall shear stress sensors must be used since Taylor's hypothesis is not valid at the wall's surface where the velocity is zero. The filtered wall shear stress obtained from the nine wall shear stress sensors will be referred to as the 'measured', τ_r , wall shear stress and it will be compared to the 'modelled', τ_m , wall shear stress obtained from the filtered velocity using equations (1), (2) and (3).

Results

SG models

Representative samples of τ_r and τ_m at $z^+ = 98$ are shown in figure 2(a). The correlation coefficient between the wall shear stress signatures,

$$R_{\tau_r\tau_m}(T) = \frac{\langle \tau_r'(t)\tau_m'(t-T) \rangle}{(\langle \tau_r'^2 \rangle \langle \tau_m'^2 \rangle)^{1/2}}, \quad (4)$$

where primes denote a fluctuating quantity, are shown in figure 2(b). T is the time delay between the two signals and both are non-dimensionalised by their rms values. The z^+ values used, except $z^+ = 311$ which is slightly beyond, correspond to positions in the boundary layer where the mean velocity profiles follow the logarithmic law of the wall. The energy spectra of the wall shear stress fluctuations are shown in 2(c),

$$\Phi_\tau(f) = \lim_{T \rightarrow \infty} \frac{1}{T} \{F.T.[\tau'(t)]F.T.[\tau'(t)]\}, \quad (5)$$

where f is frequency, $F.T[\]$ signifies the Fourier transform and $*$ indicates a complex conjugate. All spectra are normalised such that

$$\int_0^\infty \Phi_\tau(f) df = \langle \tau_r'^2 \rangle \text{ or } \langle \tau_m'^2 \rangle. \quad (6)$$

It should also be noted that $\Phi_\tau(f/f_c)$ is defined as the energy spectra per non-dimensional frequency f/f_c , where $f_c = U_c/(2\pi\delta)$ is a constant.

The high frequency oscillations in the modelled shear stress spectra seen figure 2(c), are a result the box filter but have negligible effects given the low energy content of the signals at those high frequencies. Also the step observed in the measured shear stress spectrum is an indication of some cross-correlation between the nine hot-film sensors. However, again at those frequencies the energy levels are negligible.

The disagreement between τ_r and τ_m can be seen qualitatively in figure 2(a) while figures 2(b) and (c) quantify the statistical significance of this disagreement. Figure 2(b) indicates moderate levels of agreement with the relative bluntness of the peak and the decrease in correlation with increasing distance from the wall. These findings, along with the inferred structure angles (deduced from Taylor's hypothesis, the time lag, and the wall normal distance from the wall) are consistent with the results of [9] who studied single point shear stress and velocity correlations and is suggestive of coherent structures in the turbulent boundary layer. It is because of this heightened correlation along structures (shift in time lag) that the shifted SG model was originally proposed.

A more significant discrepancy is seen in figure 2(c) with the lower energy content of τ_m . While the shapes of the

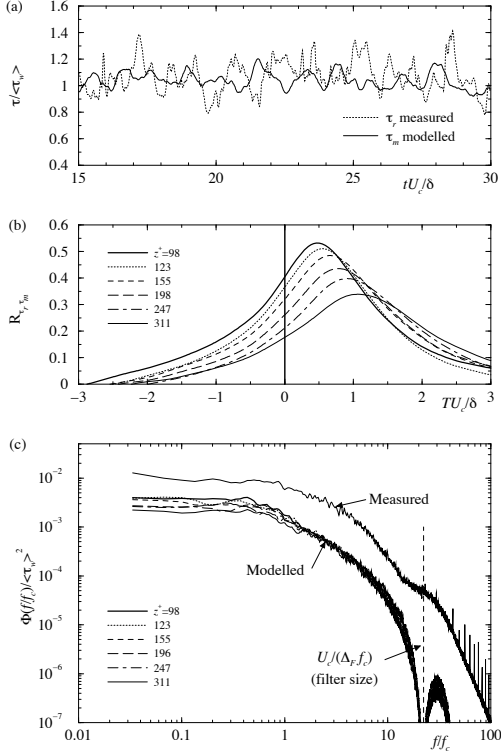


Figure 2: SG model. (a) Representative filtered wall shear stress signatures at $z^+ = 98$. (b) Correlation coefficient. (c) Energy spectra.

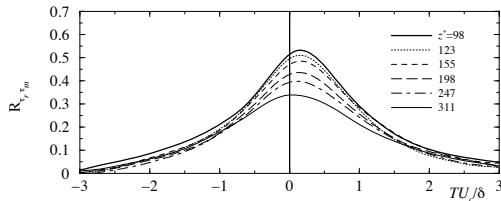


Figure 3: Shifted SG model. Correlation coefficient.

spectra are similar, the collapse of the τ_m over the range of wall normal positions is only fairly good and this may have negative consequences for the SG model when applied to higher Reynolds number flows. A solution to this is discussed in the alternative model section. Shifting the filtered velocity signature Δ_s as suggested by [7] improves the correlation of the phases of the shear stress signatures (figure 3) but has no effect on the spectra.

Ejection model

The ejection model was developed by [7] with hopes to better characterize the shear stress at the wall occurring from sweep-ejection events by using the wall-normal component of velocity. However the ejection model, seen in figure 4, less accurately predicts the wall shear stress than either of the SG models. The maximum correlation coefficients are less than 0.25, which is half as strong as the SG models, and the spectra show significant differences in shape. The τ_m -spectra (figure 4(b)) have a higher energy content at higher non-dimensional frequencies. Note that for the figures shown the dimensionless constant, C , was taken to be 0.6 which improves the agreement compared to using the suggested value of 1.0. It is uncertain

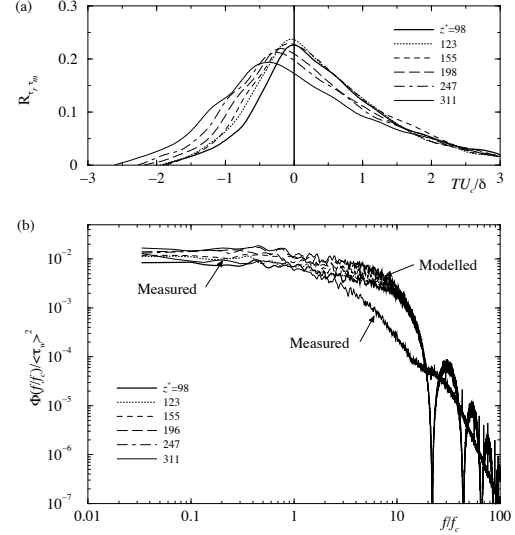


Figure 4: Ejection model. (a) Correlation coefficient. (b) Energy spectra.

if the good agreement with the ejection model suggested by [7], (DNS of channel flow at $Re_\tau = 640$) suggests that low Reynolds number effects are important. In [7] no correlation coefficient nor spectral comparisons were shown.

Alternative model

The analysis of the previous three models suggests that the streamwise component of velocity more accurately describes the wall shear stress than the wall-normal component. However, the models based on the streamwise component of velocity still show significant room for improvement. Two deficiencies have been discovered. First, they do not accurately estimate the level of energy in the wall shear stress, and second, they do not give equivalent estimates of energy content at different wall-normal positions in the logarithmic region. The latter is expected to be worse for larger Reynolds numbers. Therefore, we propose a new model based on the streamwise component of velocity,

$$\tau_m(x, y, z, t) = \langle \tau_w \rangle - \alpha U_\tau [\bar{u}(x + \Delta_s, y, z, t) - \langle \bar{u}(x, y, z, t) \rangle], \quad (7)$$

where α is a characteristic constant.

The new model was developed such that the τ_m -spectra will collapse to one curve for all positions in the logarithmic region for all Reynolds numbers. It is anticipated that the low-frequency filtered u_1 -spectra will follow standard u_1 -spectra and collapse with ‘outer-flow’ scaling ($\Phi_{u_1}(f/f_c)/(U_\tau^2) = g(f/f_c)$) [5] and that the filtering operation will collapse the data at the high frequencies. Therefore, since the filtered u_1 -spectra are expected to collapse the τ_m -spectra are expected to also. Note that using Taylor’s hypothesis with the modelled stresses implies that $f/f_c = k_1 \delta$, where k_1 is streamwise wavenumber. Results can be seen in figure 5, note that the correlation results will be the same as the shifted SG model. As seen in figure 5(b) the τ_m -spectra are shown to collapse very well. The lack of collapse at low non-dimensional frequencies is in agreement with Perry and Li [6] who suggest that it results from convection velocity variations in the use of Taylor’s hypothesis.

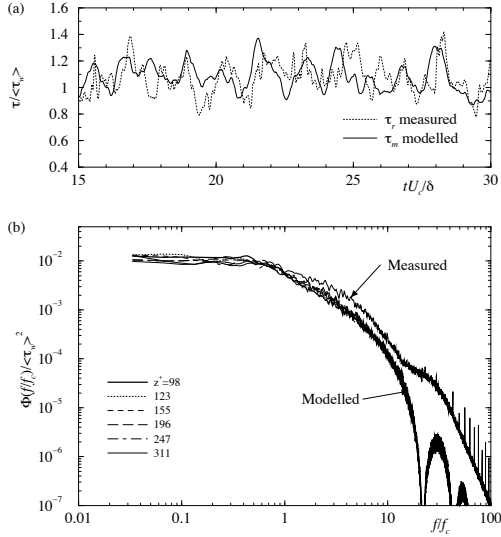


Figure 5: New model. (a) Representative filtered wall shear stress signatures at $z^+ = 98$. (b) Energy spectra.

For this attached, zero pressure gradient turbulent boundary layer the constant α has been set to 0.10. However, support for ‘outer-flow’ scaling in the logarithmic region over a range of pressure gradient flows also exists ([4] studied adverse pressure gradient flows and [3] studied favourable pressure gradient flows). The level at which the τ_m -spectra collapse is thus dependent on pressure gradient, and accordingly α has been termed a characteristic constant. Future work will determine what functional form the constant will take but current knowledge suggests its dependence on geometry and pressure gradient will be relatively weak. It should be noted that while the result in figure 5(b) show the desired collapse of the individual τ_m -spectra across the wall normal positions, the agreement with the τ_r -spectra is not complete across all the energy-containing non-dimensional frequencies. This is a limitation of using any model based solely on the streamwise velocity component alone.

Conclusions

Three existing wall boundary condition models used in Large Eddy Simulations of a turbulent boundary layer were tested. The study was confined to the streamwise component of the instantaneous wall shear stress. Consistent with a high Reynolds number simulation the first grid point (wall-normal position) was taken to be within the logarithmic region. The two models (SG and shifted SG) based on the streamwise component of velocity were found to give better estimates of the filtered wall shear stress than the ejection model, which is based on the wall-normal component of velocity.

Based on the analysis of the previous models a new model is proposed which also uses the streamwise component of velocity at the first grid point above the wall. Similar to the other models tested it is intended for attached boundary layers where the mean wall shear stresses are known. The new model incorporates the attractive features of the shifted SG model which account for inclined coherent structures near the wall and, since the streamwise component of velocity spectra follow ‘outer-flow’ scaling similarity as described by [5], the modelled spectra will likely agree with each other

for any positions within the logarithmic region at any Reynolds number. In doing so it better estimates the filtered wall shear stress than any of the other existing models tested. It is believed that this is the best model that can be proposed based on one-point information of the filtered streamwise velocity component. The proposed model is also simple enough to be used directly in existing LES codes.

References

- [1] ADRIAN, R., MENEVEAU, C., MOSER, R. & RILEY, J., Final report on ‘Turbulence Measurements for LES’ workshop. *Tech. Rep.*, 2000, 937. Theoretical and Applied Mathematics, University of Illinois at Urbana-Champaign.
- [2] GRÖTZBACH, G., Direct numerical and large eddy simulations of turbulent channel flows. *Encyclopedia of Fluid Mechanics* **6**, 1987, 1337–1391.
- [3] JONES, M. B., MARUSIC, I. & PERRY, A. E., Evolution and structure of sink flow turbulent boundary layers. *J. Fluid Mech.* **428**, 2001, 1–27.
- [4] MARUSIC, I. & PERRY, A. E., A wall-wake model for the turbulence structure of boundary layers. Part 2. Further experimental support. *J. Fluid Mech.* **298**, 1995, 389–407.
- [5] PERRY, A. E., HENBEST, S. M. & CHONG, M. S., A theoretical and experimental study of wall turbulence. *J. Fluid Mech.* **165**, 1986, 163–199.
- [6] PERRY, A. E. & LI, J. D., Theoretical and Experimental studies of shear stress profiles in two dimensional turbulent boundary layers. *Rep. FM-18*. Dept. of Mech. Eng., University of Melbourne, 1991.
- [7] PIOMELLI, U., FERZIGER, J. & MOIN, P., New approximate boundary conditions for large eddy simulations of wall bounded flows. *Phys. Fluids A* **1(6)**, 1989, 1061–1068.
- [8] PORTÉ-AGEL, F., PARLANGE, M. B., MENEVEAU, C. & EICHINGER, W. E., A priori field study of the subgrid-scale heat fluxes and dissipation in the atmospheric surface layer. *J. Atmos. Sci.* In press, 2001.
- [9] RAJAGOPALAN, S. & ANTONIA, R., Some properties of the large structure in a fully developed turbulent duct flow. *Phys. Fluids* **22(4)**, 1979, 614–622.
- [10] SCHUMANN, U., Subgrid scale model for finite difference simulations of turbulent flows in plane channels and annuli. *J. Comp. Phys.* **18**, 1975, 376–404.